

Influence of pulse width on decolorization efficiency of organic dye by discharge inside bubble in water

S Kawano¹, K Wada¹, T Kakuta¹, K Takaki^{1,2}, N Satta³ and K Takahashi⁴

¹ Faculty of Engineering, Iwate University, 4-3-5, Ueda, Morioka, Iwate 020-8551, Japan

² Soft-Path Engineering Research Center (SPERC), Iwate University, 4-3-5, Ueda, Morioka, Iwate 020-8551, Japan

³ Faculty of Agriculture, Iwate University, 3-18-8, Ueda, Morioka, Iwate 020-8550, Japan

⁴ Shishido Electrostatic, LTD., 4-7-21, Chigasaki-higashi, Tsuzuki-ku, Yokohama, Kanagawa 224-0033, Japan

Email: takaki@iwate-u.ac.jp

Abstract. Decolorization of an organic dye by discharge in high conductive water using a pulsed power generator and a discharge reactor was investigated. The discharge reactor consisted of a glass tube and a tungsten wire inserted into the glass tube, which was immersed in the water. Room air was injected into the glass tube to generate bubbles in the water. High voltage pulses were generated by an inductive-energy storage system using semiconductor opening switch (SOS) and by a magnetic pulse compression circuit. Fast recovery diodes were used as SOS diode in the inductive-energy storage system. The pulse width was changed in range from 10 to 1200 ns. The high voltage was applied to the tungsten wire. Indigo carmine was employed as a specimen to evaluate decolorization efficiency. Potassium nitrate was used to adjust the solution conductivity. The dye solution was successfully decolorized at 7 mS/cm conductivity. Energy efficiency for decolorization increased from 0.680 to 55.6 mg/Wh with decreasing the pulse width from 1200 to 10 ns owing to the reduction of ohmic loss.

1. Introduction

Water treatment using methods such as filtration, chemical oxidation and bioremediation has been used at a treatment of organic compounds in water [1]. Filtration techniques are widely used because of the high performance, while concentrated waste disposal remains. Chemical oxidation using chlorine and ozone has been shown to produce hazardous by-products such as trihalomethanes, aldehydes and bromate [2, 3]. Ozone is a weaker oxidizing agent than hydroxyl radical and rather selective oxidant. Ozone oxidation and Bioremediation are limited by slow kinetics. A pulsed discharge plasma for treating pollutants in water has been attracted much attention [4]. The production of discharge plasmas with large volume discharge requires pulsed power technologies because the discharges in water demands high electric field. The pulsed discharge makes it possible to instantaneously produce a non-thermal plasma in which various chemical species such as hydroxyl radical exist. These species play important role in degradation of chemical organic compounds [5-7].

In general, an energy efficiency for the degradation of chemical organic compounds in water decreases with increasing conductivity of the water [6-10], because of an increase of energy



dissipation by the ohmic loss which doesn't contribute to production of the chemical species [10]. As the result, the energy efficiency for water treatment by the discharge decreases to be low at high conductivity. To solve this problem, gas-liquid separated reactors and short pulse generators have been proposed [7, 11]. The short pulse can produce ozone with high energy efficiency because of a decrease the conductive current [12].

Objective of the present work is to clarify an influence of the pulse width on energy efficiency to decolorize high-conductive solution using pulsed discharge inside bubble. Indigo carmine is employed as specimen to evaluate the energy efficiency. The high voltage pulses are generated by an inductive-energy storage system using semiconductor opening switch (SOS-IES) and by a magnetic pulse compression circuit (MPC). The pulse width is adjusted in range from 10 to 1200 ns. The solution conductivity is adjusted in range from 6 to 7000 $\mu\text{S}/\text{cm}$ by mixing potassium nitrate.

2. Experimental setup and procedure

Figure 1 shows a schematic diagram of the pulsed power generator with IES using SOS. The pulsed power generator is consisted of a capacitor C_0 , gap switch, a pulsed transformer P.T. (Hitachi Metals, Ltd., FT-3L), primary energy storage capacitor C_1 , secondary energy storage inductor L_2 , resistor R_C and fast recovery diode (Voltage multiplier, K100UF). Fast recovery diodes are used as semiconductor opening switch (SOS). When the gap switch is closed, the energy stored in C_0 is transferred to C_1 through the pulse transformer. The pulsed voltage is generated by LC oscillation in the secondary circuit. The SOS diode is pumped up with forward current in half cycle determined by the inductance L_2 by capacitance C_1 . After the half cycle, the current direction changes to reversed direction of the SOS diode. The reversed current is interrupted rapidly by the SOS diode, as the result, the pulse voltage appears between the inductor. The pulse width is controlled to be 10 or 65 ns by adjusting L_2 . Figure 2 shows typical waveforms of the output voltage (v_o) without connection to the reactor. The pulse width of the output voltage is 10 ns without external inductor L_2 and increases to 65 ns with external inductor L_2 at 16.2 μH .

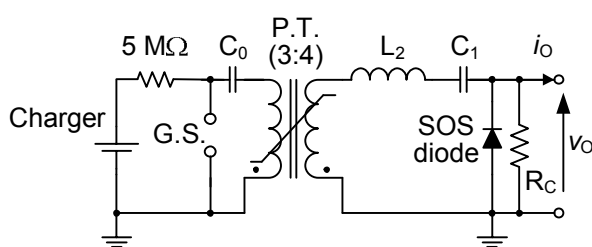


Figure 1. Schematic diagram of the IES pulsed power generator using SOS; $C_0 = 2.3 \text{ nF}$, $C_1 = 0.5 \text{ nF}$, $L_2 = 0$ or $16.2 \mu\text{H}$, $R_C = 20 \text{ k}\Omega$.

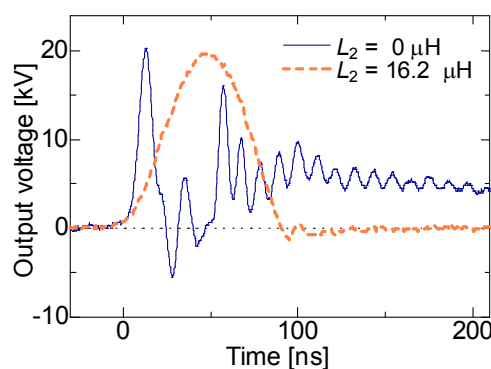


Figure 2. Waveforms of the output voltage of the IES pulsed power generator using SOS without the reactor; $L_2 = 0$ or $16.2 \mu\text{H}$.

Figure 3 shows a schematic diagram of the magnetic pulse compression circuit (Suematsu Electronics CO., LTD., MPC-3000S SP). The capacitor C_0 is charged up to a charging voltage by the charger. The energy stored in C_0 is transferred to C_1 through the pulse transformer P.T. The pulsed voltage is produced at secondary side of the pulse transformer. The pulsed voltage is compressed by saturable inductors (SI_1 , SI_2 and SI_4) and capacitors (C_2 and C_3). SI_3 is connected in parallel with C_3 to shorten the pulse width of the output voltage (v_o). The output voltage is rectified by the diode connected to the output terminal. Figure 4 shows typical waveforms of the output voltage (v_o) without connection to the reactor. The pulse width of the output voltage is 400 ns with SI_3 and is 1200 ns without SI_3 in condition of no load condition.

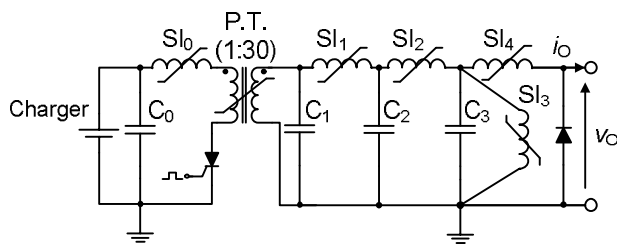


Figure 3. Schematic diagram of a magnetic pulse compression circuit; $C_0 = 2.24 \mu\text{F}$, $C_1 = C_2 = 2 \text{ nF}$, $C_3 = 0.7 \text{ nF}$.

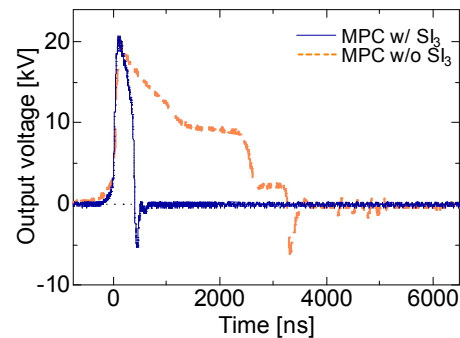


Figure 4. Waveforms of output voltage of the magnetic pulse compression with Sl_3 and without Sl_3 in condition of no load.

Figure 5 shows a schematic diagram of the discharge reactor. A glass tube containing a stainless steel wire and four glass tubes containing a tungsten wire are immersed in glass beaker (100 mm height, 50 mm diameter) as shown in the figure 5. The inner diameter of the glass tubes is 0.8 mm. The stainless steel wire (0.2 mm diameter) is a ground electrode and is immersed water. The gap length between tip of the ground electrode and tip of the glass tube is 15 mm. Room air is injected into the reactor through another four glass tubes with the gas flow rate in 2 L/min. The gap length between the tip of the tungsten wire and tip of the glass tube is 20 mm. The pulse voltage v_0 generated by pulsed power generators is applied to the tungsten wires to generate streamer discharge in the tubes and air bubbles. The output voltage v_0 of the pulse generator has peak value of 20 kV. A pulse repetition rates is controlled to be 80 pulses per second.

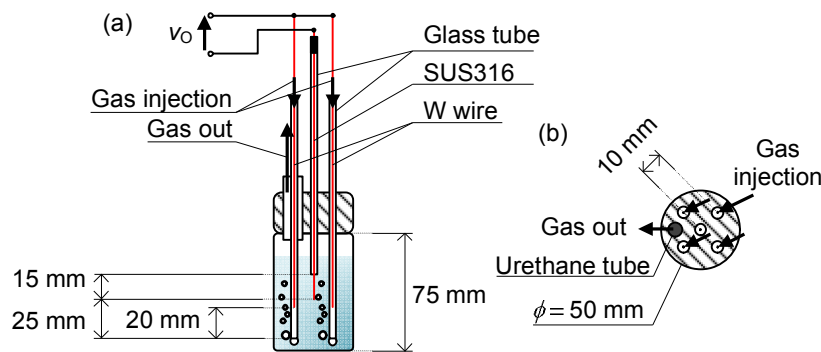


Figure 5. Schematic diagram of the reactor; (a) side view, (b) top view.

A dye solution dissolving indigo carmine (CAS No. 860-22-0) into 100 ml of purified water at concentration of 10 mg/L is used to evaluate by a decolorization efficiency. The initial pH of the solution is 5.5. The electrical conductivity (σ) is adjusted in range from 6 to 7000 $\mu\text{S/cm}$ by mixing potassium nitrate. The absorbance of the dye solution is measured by a spectrometer (Milton Roy Ltd., Spectronic 301) and the decolorization rate (DR) is obtained by following equation,

$$DR = \frac{\text{Absorbance (initial)} - \text{Absorbance (treated)}}{\text{Absorbance (initial)}} \times 100[\%], \quad (1)$$

where the absorbance is obtained at 610 nm in wavelength. The energy efficiency for decolorization of the indigo carmine (ED) is obtained by following equation,

$$ED = \frac{DR \times 36}{J_T} [\text{mg/Wh}], \quad (2)$$

where J_T is total input energy into the reactor calculated by output voltage and current.

3. Experimental Results

Figure 6 shows the decolorization rate as a function of the treatment time for various pulse widths at 6 $\mu\text{S/cm}$ in initial conductivity. The energies per a pulse are 3.45, 2.61, 2.49 and 3.68 mJ at 10, 65, 400 and 1200 ns in pulse width, respectively. The decolorization rate increases with increasing the treatment time. The treatment time at almost 100% decolorization increases with increasing pulse width. The treatment times of 100% decolorization are 5.0, 6.5, 7.0 and 8.5 min at 10, 65, 400 and 1200 ns in pulse width, respectively. The energy efficiencies of 50% decolorization are 100, 88, 83 and 55 mg/Wh at 10, 65, 400 and 1200 ns in pulse width, respectively.

Figure 7 shows the decolorization rate as a function of treatment time for various pulse widths at initial conductivity of 7000 $\mu\text{S/cm}$. The energies per a pulse are 6.14, 22.9, 56.0 and 160 mJ at 10, 65, 400 and 1200 ns in pulse width, respectively. The treatment times of 100% decolorization are 4.5 and 4 min at 10 and 65 ns in pulse width, respectively. These values are lower than that at 6 $\mu\text{S/cm}$. On the other hand, the treatment time of 100% decolorization at 7000 $\mu\text{S/cm}$ is much larger than that at 6 $\mu\text{S/cm}$ in the case of 400 and 1200 ns pulse widths. The energy efficiencies of 50% decolorization are 55.6, 38.1, 4.32 and 0.680 mg/Wh at 10, 65, 400 and 1200 ns in pulse width, respectively.

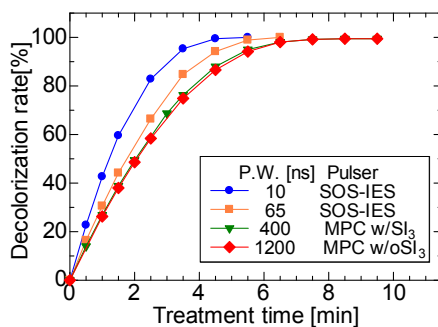


Figure 6. Decolorization rate as a function of treatment time for various pulse widths at 6 $\mu\text{S/cm}$.

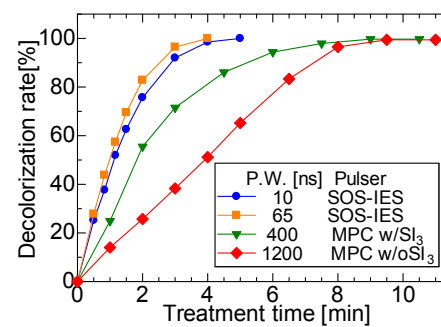


Figure 7. Decolorization rate as a function of treatment time for various pulse widths at 7000 $\mu\text{S/cm}$.

Figure 8 shows the decolorization rate as a function of initial conductivity for various pulse widths. The decolorization rate at 6 $\mu\text{S/cm}$ is controlled to be 22% by changing the treatment time. The treatment time t_t are 30, 40, 60 and 60 s at 10, 65, 400 and 1200 ns in pulse width, respectively. The decolorization rate increases with increasing conductivity at 10 ns in pulse width. On the other hand, the decolorization rate decreases rapidly at 2000 and 1000 $\mu\text{S/cm}$ conductivity in the case of 400 and 1200 ns in pulse width, respectively. Figure 9 show the energy efficiency for decolorization as a function of conductivity in solution for various pulse widths. The energy efficiency for decolorization increases with decreasing pulse width.

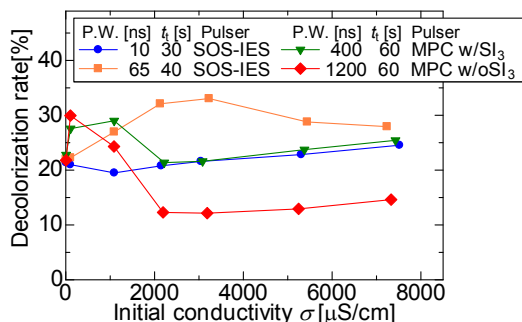


Figure 8. Decolorization rate as a function of initial conductivity for various pulse widths.

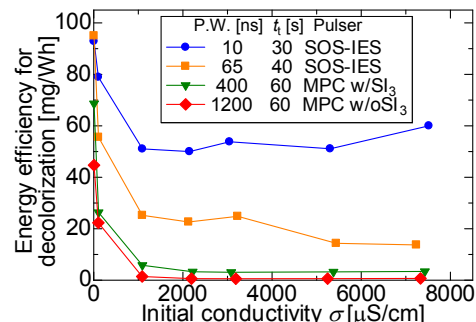
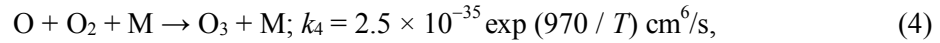
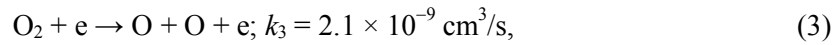


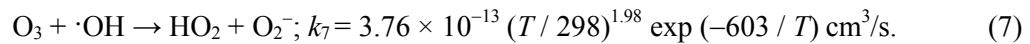
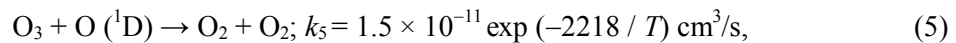
Figure 9. Energy efficiency as a function of initial conductivity for various pulse widths.

4. Discussion

Indigo carmine has high reactivity with ozone [13]. Active species such as ozone (O_3) and oxygen atom (O) are generated by discharge inside air bubbles through the reactions and reaction rates in following equations (3) and (4) [14-16],



where M is the third collision partner and T is the temperature of gas; M takes part in energy absorption, but does not react chemically. Reaction of equation (3) increases with increasing discharge energy [12]. Reaction of equation (4) decreases by increasing T . In figure 8, decreasing the decolorization rate in the condition of the pulse width of 65, 400 and 1200 ns is caused by decreasing amount of ozone generation due to increasing temperature of gas. In addition, ozone is consumed by various reactions because of its high reactivity, as shown in following equations (5) and (6) [13, 5-17],



Reactions of equations (5-7) increase with increasing temperature of gas and discharge. Amount of ozone generation is decreased by increasing temperature of gas and discharge.

Figure 10 shows concentration of ozone exhausted from the reactor as a function of conductivity in the solution. The purified water is used instead of the indigo carmine solution. The ozone concentration increases by early increase conductivity, in the case of the pulse width of 10 and 65 ns. On the other hands, it drastically decreases at 1000 $\mu\text{S}/\text{cm}$ conductivity in the case of 400 and 1200 ns in pulse width. This decrease is similar to the decrease of the decolorization rate at 400 and 1200 ns in pulse width as shown in figure 8. The ozone concentration at 65 ns in pulse width is higher than 10 ns, because energy per a pulse in 65 ns is higher than 10 ns, for example energy per a pulse in 65 and 10 ns at 7000 $\mu\text{S}/\text{cm}$ are 6.14 and 22.9 mJ, respectively. And temperature of gas and discharge increase to 1000 K from 450 K at 10 and 65 ns in pulse width [18, 19]. Therefore, reactions of equations (5-7) hardly increase. In figure 8, the decolorization rate at 65 ns in pulse width is higher than 10 ns. It is same reason in the case of the ozone concentration.

Figure 11 shows the normalized energy per a pulse as a function of initial conductivity for various pulse widths. The normalized energy is obtained as energies divided by the energy of 6 $\mu\text{S}/\text{cm}$ in conductivity. The normalized energy increases with increasing pulse width. The streamer discharge propagates from the tip of wire electrode to the surface of bubble [20]. After the streamer discharge reach to surface of the bubble, the output current increases rapidly because of thermalization of the discharge plasma. The amplitude of the discharge current after the plasma thermalization increases

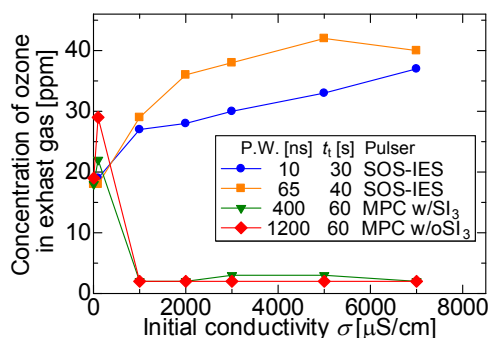


Figure 10. Concentration of ozone in exhaust gas as a function of initial conductivity for various pulse widths.

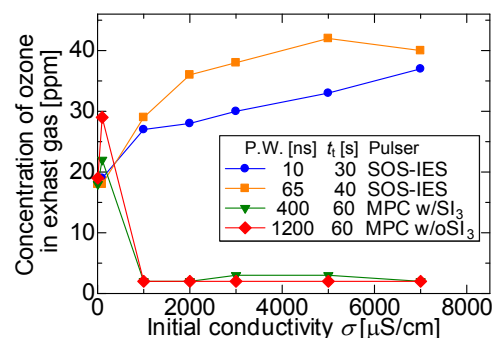


Figure 11. Normalized energy per a pulse as a function of initial conductivity for various pulse widths.

with conductivity because the discharge current is limited by resistance of the water [21, 22]. The consumed energy can also be reduced by shorten the pulse width. As the results, the energy efficiency for decolorization is strongly affected by not only water conductivity but also the pulse width.

5. Conclusion

The water decolorization was carried out at four different pulse widths using two types of the pulse generator. The indigo carmine solutions were decolorized completely by discharge. The time demand for complete decolorization of the dye decreased with decreasing pulse width. The energy efficiency was improved by decreasing pulse width. The short pulse width was effective for high conductive water treatment.

Acknowledgments

The authors are grateful to Dr. Shoji Koide, Faculty of Agriculture, Iwate University and Mr. Ippei Yagi, The University of Tokyo. This work was supported by Grants-in-Aid for Scientific Research (JSPS fellowship No. 20380130).

References

- [1] Vandevivere P C, Bianchi R and Verstraete W 1998 *J. Chem. Thechnol. Biotechnol.* **72** pp 289-302
- [2] Richardson S D, Thruston A D, JR, Caughran T V, Chen P H, Collette T W, Schenck K M, Lykins B W, JR, Rav-Acha C, Glezer V 2000 *Water Air Soil Poll.* **123** pp 95-102
- [3] Gunten U V, Hoigné J 1994 *Environ. Sci. Technol.* **28** pp 1234-1242
- [4] Akiyama H, Sakugawa T, Namihira T, Takaki K, Minamitani Y and Shimomura N 2007 *IEEE Trans. Dielect. Electr. Insul.* **14** pp 1051-1063
- [5] Sato M, *Plasma Sources Sci. Technol.* 2008, **17**, 024021 pp 1-7
- [6] Akiyama H. *IEEE Trans. Dielect. Electr. Insul.* 2000 **7** pp 646-653
- [7] Takahashi K, Takaki K and Satta N 2012 *J. Adv.Oxidat.* **15** 2 pp 365-373
- [8] Clements J S, Sato M and Davis R H 1987 *IEEE Trans. Ind. Appl.* **IA-23** 2 pp 224-235
- [9] Lukes P, Clupek M, Babicky V and Sunka P 2008 *Plasma Sources Sci. Technol.* **17** 024012 pp 1-11
- [10] Dang T H, Denat A, Lesaint O and Teissedre 2008 *Plasma Sources Sci. Technol.* **17** 024013 pp 1-8
- [11] Malik M A 2010 *Plasma Chem. Plasma Proc.* **30** pp 21-31
- [12] Matsumoto T, Wang D, Namihira T and Akiyama H 2010 *IEEE Trans. Plasma Sci.* **38** 1 pp 2639-2643
- [13] Criegee R 1975 *Angew. Chem. Internat. Edit.* **17** 11 pp 745-752
- [14] Chang J S, Lawless A Phill and Yamamoto T 1991 *IEEE Trans. Plasma Sci.* **19** 6 pp 1152-1166
- [15] Yanallah K , Ziane S H, belasri A and Meslem Y 2006 *J. Mol. Struct.* **777** pp 125-129
- [16] National Institute of Standards and Technology last modified February 2012 <http://kinetics.nist.gov/kinetics/index.jsp>
- [17] Locke B R and Thagard S M 2009 *IEEE Trans. Plasma Sci.* **37** 4 pp 494-501
- [18] Namihira T, Wang D, Matsumoto T, Okada S and Akiyama H 2009 *IEEE Trans. FM* **129** 1 pp 7-14
- [19] Kawano S, Takahashi K, Takaki K, Satta N 2012 *J. Inst. Electrostat. Jpn.* **36** 1 pp 43-49
- [20] Takahashi K, Yagi I, Takaki K and Satta N 2011 *IEEE Trans. Plasma Sci.* **39** 11 pp 2654-2655
- [21] Yoshinaga K, Okada S, Wang D, Namihira T and Akiyama H 2009 *the 2nd Euro-Asian Pulsed Power Conference* **115** 6 pp 1050-1052
- [22] Bruggeman P, Ribežl E, Maslani A, Degroote J, Malesevic A, Rego R and Leys C 2008 *Plasma Sources Sci. Technol.* **17** 025012 pp 1-10